Computers and Chemical Engineering 141 (2020) 107001

Contents lists available at ScienceDirect

Computers and Chemical Engineering

journal homepage: www.elsevier.com/locate/compchemeng

Can the operating limits of biogas plants operated under non-isothermal conditions be defined with certainty? Modeling self-optimizing attainable regions

F. Abunde Neba[a,d,e,*], Michel Tornyeviadzi[a,e], Nana Y. Asiedu[c], Ahmad Addo[b], John Morken[f], Stein W. Østerhus[d], Razak Seidu[e]

[a] Abunde Sustainable Engineering Group, (AbundeSEG), Cameroon
[b] Department of Agricultural and Biosystems Engineering, Kwame Nkrumah University of Science and Technology, Kumasi, Ghana
[c] Department of Chemical Engineering, Kwame Nkrumah University of Science and Technology, Kumasi, Ghana
[d] Department of Civil and Environmental Engineering, Norwegian University of Science and Technology, Trondheim, Norway
[e] Department of Marine Operations and Civil Engineering, Norwegian University of Science and Technology, Ålesund, Norway
[f] Faculty of Science and Technology, Drobakveien 31, 1432 Aas, Norwegian University of Life Sciences, Ås, Norway

ARTICLE INFO

Article history:
Received 18 October 2019
Revised 31 January 2020
Accepted 29 June 2020
Available online 30 June 2020

KeyWords:
Self-optimizing operating limits
Attainable regions
Process kinetics
Biogas digesters
Temperature

ABSTRACT

Uncertainty in operating parameters such as temperature undermines the reliability of using kinetic models in performance projections for plants operated under ambient non-isothermal conditions. This study develops a theoretical framework, which uses process kinetics, uncertainty quantification to define robust operating limits known as self-optimizing attainable regions, where by instead of defining a very large operating limit, which will be achieved some of the times for some of the reactor configurations, we define a self-optimizing limit, which will be achieved all the times for all possible reactor configurations (despite variations in temperature). Using a temperature range of 20 – 60$^{\circ}C$, , the results indicate that decreasing temperature uncertainty, increasing process temperature or using a multistage digester structure increases the self-optimizing operating limits: 1.53×10^{-4}, 4.95×10^{-4} and 6.32×10^{-4} $(g/L)^2$ obtained for temperatures of 20.00, 31.60 and 52.40$^{\circ}C$ respectively. The findings highly important in defining performance targets especially when there is uncertainty in environmental conditions.

1. Introduction

Environmental pollution resulting from the use of fossil fuels coupled with potential exhaustion of fossil fuel resources makes it necessary to find alternative energy sources that are renewable and environmentally sustainable. Biogas, a methane-rich renewable energy obtained from the anaerobic treatment of organic wastes has proven to have a great potential in shifting reliance on fossil-based energy. However, biogas production from anaerobic digestion is influenced by a myriad of factors including substrate characteristics and concentration, presence of inhibitory substances as well as temperature and pH and reactor configurations (Henze et al., 2008; Wang et al., 2007). Amongst these factors, temperature is considered very important, since it influences the activity of anaerobic microorganisms by influencing the activity of some essential enzymes involved in organic matter degradation and biogas production (Kim et al., 2017; Donoso-Bravo et al., 2013). Biogas plants can generally be operated under four temperature regimes depending on the type of microorganisms present: psychrophilic digestion (15–25$^{\circ}C$), mesophilic digestion (30–40$^{\circ}C$), thermophilic digestion (50–60 $^{\circ}C$) and hyper-thermophilic (65–75 $^{\circ}C$) digestion (Kuo and Lai, 2010; Wang et al., 2012; Saady and Massé, 2015; Pavlostathis and Giraldo-Gomez, 1991). Within each of the temperature regimes, the activity of anaerobic microorganisms increases with increasing temperature up to a maximum activity above which a sharp drop is observed with increase in temperature (Pavlostathis and Giraldo-Gomez, 1991). In terms of capacity, biogas plants can usually be operated as large-scale (common in the developed world) or small-scale (common in developing countries) systems. The large-scale systems are normally operated under controlled isothermal conditions (most commonly at mesophilic or thermophilic regimes). This implies that the influence of the temperature on large-scale plants can be considered constant (Donoso-Bravo et al., 2013), and hence the performance of large-scale sys-

* Corresponding author.
E-mail address: fabricen@stud.ntnu.no (F. Abunde Neba).

https://doi.org/10.1016/j.compchemeng.2020.107001

Nomenclature

$(VS)_0$	Initial concentration of volatile solids ($g\,VS/L$)
A_f	Acidity factor ($g\,VFA/L$)/($g\,BVS/L$)
B_0	Biodegradability constant ($g\,BVS/L$)/($g\,VS/L$)
$K_{i_{me}}$	VFA inhibition constant for methanogenic archae ($g\,VFA/L$)
$K_{s_{ac}}$	Monod half-saturation constant for acidogenic bacteria ($g\,BVS/L$)
$K_{s_{me}}$	Monod half-saturation constant for acidogenic bacteria ($g\,VFA/L$)
S_{BVS_0}	Initial concentration of biodegradable volatile solids ($g\,BVS/L$)
S_{BVS}	Concentration of biodegradable volatile solids ($g\,BVS/L$)
S_{VFA_0}	Initial concentration of volatile fatty acids ($g\,VFA/L$)
S_{VFA}	Concentration of volatile fatty acids in bioreactor ($g\,VFA/L$)
$T_{\max}$	Maximum temperature at which growth rate is zero ($^\circ C$)
$T_{\min}$	Minimum temperature at which growth rate is zero ($^\circ C$)
X_0	Initial concentration of biomass in reactor (g/L)
X_{ac_0}	Initial concentration of acidogenic bacteria ($g\,ac./L$)
X_{ac}	Concentration of acidogenic bacteria in bioreactor ($g\,ac./L$)
X_{me_0}	Initial concentration of methanogenic archaea ($g\,me./L$)
X_{me}	Concentration of methanogenic archaea in bioreactor ($g\,me./L$)
k_1	Yield constant ($g\,BVS/g\,ac./L$)
k_2	Yield constant ($g\,VFA/g\,ac./L$)
k_3	Yield constant ($g\,VFA/g\,me./L$)
$r_{S_{BVS}}$	Reaction rate for biodegradable volatile solids ($g\,BVS/L/d$)
$r_{S_{VFA}}$	Reaction rate for volatile fatty acids ($g\,VFA/L/d$)
$r_{X_{ac}}$	Reaction rate for acidogenic bacteria ($g\,ac./L/d$)
$r_{X_{me}}$	Reaction rate for methanogenic archae ($g\,me./L/d$)
$t_{\upsilon,\alpha/2}$	Student t-distribution parameter
$\hat{\beta}$	Vector of estimated model parameters
γ_{CH_4}	Volumetric methane productivity ($L\,CH_4/m^3/d$)
γ_s	Methane yield
$\mu_{m_{ac}}$	Maximum specific growth rate of acidogenic bacteria (d^{-1})
$\mu_{m_{me}}$	Maximum specific growth rate of methanogenic archaea (d^{-1})
μ_{ac}	Specific growth rate of methanogenic archaea (d^{-1})
μ_{me}	Specific growth rate of methanogenic archaea (d^{-1})
σ^2	Standard error
B	Ratkowsky parameter ($^\circ C^{-1}\ h^{-0.5}$)
C	Ratkowsky parameter C ($^\circ C^{-1}$)
T	Reactor temperature ($^\circ C$)
EMY_{90}	90% experimental methane yield ($mL\,CH_4/gVS$)
$HRT(T_{90})$	Hydraulic retention time that gives 90% experimental methane yield (d)
J	Jacobian matrix evaluated at parameter estimates
VSL	Volatile solids loading (gVS/l)
VSR	Volatile solids reduction (%)
n	Number of experimental data points
p	Number of model parameters
α	Significance level
β	Vector of real model parameters
ϑ	Acidogenic fraction

tems can more closely mimic theoretical predictions during economic feasibility studies, which use projections in biogas production corresponding to a fixed temperature. On the other hand, small scale systems (such as domestic biogas septic tanks) are mostly operated under ambient non-isothermal conditions (mostly due to cost constraints), where heating of high volumes of organic waste is unlikely (Bandara et al., 2012; Sumino et al., 2007). Small scale plants operated under these non-isothermal conditions are usually viable to uncertain performance resulting from temperature fluctuations mainly due to seasonal variations, day–night patterns as well as specific spikes or drops events. This makes the definition of operating limits a challenging task for small scale systems as large performance deviations are usually observed between predicted and actual. There have been several studies investigating the influence of temperature on the performance of the anaerobic treatment process examining microbial community (Kim et al., 2017), organic matter removal (Lohani et al., 2018), biogas production (Li et al., 2013; Latif et al., 2012) and digester configuration (Chong et al., 2012). The studies investigating the effect of temperature on the performance of anaerobic digestion generally proceed by four main steps: (1) Defining a digester configuration or list of digester configurations to be tested, (2) defining a list of temperatures within the psychrophilic, mesophilic or thermophilic range (3) evaluating the process performance (e.g. organic matter removal, biogas production or nutrient recovery) for the defined temperatures and digester configurations (4) Making a decision on which temperature gives the best performance for which digester configuration. The results of such studies are only relevant to industrial scale projections where temperature is usually controlled, and the optimal solution is most probably a local optimum since it is selected from the options predefined in steps (1) and (2). What if other digester configurations exist that could perform better for temperatures not considered? Several configurations of anaerobic digesters have been developed aimed at enhancing the performance of the treatment process with regards to biogas production or organic matter removal. A generalized classification of anaerobic digesters configurations fall under three main groups: single-stage systems, multi-stage systems, and hybrid systems such as electrochemical anaerobic digesters (De Vrieze et al., 2018), solar bio-hybrid digesters (Bustamante and Liao, 2017), etc. Amongst the aforementioned configurations, several studies have reported the multiple-staged systems to be the most promising technology in terms of flexibility and ability to optimize every step of the anaerobic digestion process (Akobi et al., 2016; Zhang et al., 2017). In multistage digestion systems, the concept is to stage the anaerobic digestion process based on kinetic and physiological differences between the different groups of microorganisms catalysing the different stages of the AD process (EPA, 2006). Most research on staged anaerobic digestion has focused on comparative analysis between single and multiple stage anaerobic digesters, with less effort geared towards obtaining an optimal staging configuration. While the performance advantages of multistage anaerobic systems as opposed to single staged have been well established, there is lack of a systematic digester design approaches that considers the temperature variations on the performance multistage systems. Current approaches are empirical, involving experimental evaluation of predefined configurations of different temperatures, which is not only time consume and expensive, but also results in a local optimum. An approach to determine the performance targets for all possible temperature variations and for all possible digester configurations will therefore be a breakthrough to sup-

port investment decisions in biogas plants operated under non-isothermal conditions.

Unlike conventional studies that would proceed by evaluating the effect of temperature on a given digester configuration, we rather proceed by defining the performance targets for all possible digester configurations and for all possible temperature fluctuations. The current study discusses how the attainable region concept could be used for performance targeting and digester synthesis under non-isothermal plant operation. The attainable region (AR) represents a collection of all possible outputs for all possible process configurations by interpreting processes as geometric objects that define the operating limits without having to explicitly enumerate all possible design configurations (Hildebrandt and Glasser, 1990; Hildebrandt et al., 1990; Ming et al., 2013; Ming et al., 2016). Our recent studies, have been first of their kind illustrating the usefulness of AR to model digester configurations that optimize methane productivity and volatile solids reduction (Abunde Neba et al., 2019c) as well as stability of methanogenic archaea (Abunde Neba et al., 2019b). Both studies put together have illustrated that a change in the kinetic model structure or value of kinetic coefficients, induced by differences in substrate and inoculum characteristics significantly influences the performance target as well as the optimal digester configuration required to achieve the target. In another recent study, the authors demonstrated the coupling of attainable regions and fuzzy multicriteria decision making for synthesis of high rate digesters without any need for a kinetic model (Abunde Neba et al., 2019d). Also, a framework for coupling simplified kinetic models and economic feasibility indicators for synthesis of digester structures using attainable regions have been demonstrated by the authors (Abunde Neba et al., 2019a). The studies were able to define the absolute best performance for all possible digester configurations considering mixing and reaction as fundamental processes occurring in the digester. However the studies assumed isothermal conditions where the attainable region are defined at a given operating temperature and is therefore well suited for industrial scale operation where temperature is controlled. In the current study, we seek extend the previous works by presenting the limits of achievability for non-isothermal biogas plants i.e. biogas plants operated under thermal uncertainty. We introduce the concept of self-optimizing operation, an attainable region or performance target that results in near optimal operation in spite of temperature fluctuations within the process. A self-optimizing operation (Gausemeier et al., 2006; Permin et al., 2016) is when we can achieve an acceptable loss performance by using constant setpoint values for operating parameters (e.g. temperature, kinetics, substrate characteristics, etc.,) without the need to reoptimize when variations occur. Since the AR theory involves mixing and attainability of states under defined conditions of temperature, feed composition and kinetics, the idea behind this study is to model the uncertainty in state predictions resulting from temperature fluctuations and propagate this uncertainty onto the attainable regions to define the self-optimizing attainable regions. Unlike the attainable regions, which are valid for defined temperatures, the self-optimizing attainable regions (though results in acceptable loss in performance) is valid for all possible temperatures within a defined rage.

2. Materials and methods

This study applies a proactive approach of dealing with thermal uncertainty, where by before defining the limits of achievability of the system (constructing the attainable regions), we first quantify the model prediction uncertainty resulting from the temperature variations. Three different uncertainty bounds (the 10th percentile, mean and the 90th percentile) are used to construct three sets of attainable regions and the region of intersection between these three sets represents the limits of achievability (performance targets) of the system under non-isothermal conditions. Finally we apply the necessary conditions of attainable regions to interpret the boundaries of the intersection region into digester configurations. To better illustrate the methods, given an organic substrate to be used as feedstock for biogas production, Fig. 1 outlines the work flow needed to define the maximum design and performance targets for a given anaerobic treatment process.

The following steps provide more detailed description and/or rational behind each of the steps presented in the methodological workflow (Fig. 1).

2.1. Organic substrate and characteristics

The targets of biogas production depends on both the plant design and the feedstock characteristics. The scope of this study is on plant design and considers that the substrate as well as its characteristics and potential to produce biogas are known. The organic substrate considered for the anaerobic digestion process is diary manure, which was digested with the following experimental characterization (Kafle and Chen, 2016): $HRT\ \ (T_{90}) = 28days,\ EMY = 204mL/gVS,\ 90\%\ EMY = 18.6mL/gVS,\ VSL = 3.5gVS/l,\ VSR = 58.6\%$. The data was utilized to calculated the volumetric methane production rate ($\gamma_{CH_4} = 2.95l/m^3/d$) required for the modeling framework presented in this study. The formulae applied for calculations are as presented in our previous study (Abunde Neba et al., 2019c).

$$\gamma_{CH_4} = \frac{EMY_{90}}{HRT} \times VSL \tag{1}$$

2.2. Modeling the anaerobic treatment process

The geometric optimization technique of attainable regions utilized in this study is based on the process kinetics. Because the geometric calculations (such as rate vectors, CSTR locus, PFR trajectories) are complex (will be explained further in Section 3.2.3), it is required to use a simplified model of the anaerobic treatment process, which present a compromise between being highly accurate but very complex input requirement and highly simplified but very limited predictive ability. In addition, because we are dealing with non-isothermal conditions, the normal Arrhenius equation widely use to model temperature dependence will not be appropriate as it only reproduces the increasing part of the temperature influence on the activity of anaerobic microorganisms meanwhile the activity of microorganisms drop significantly after reaching an optimum (Pavlostathis and Giraldo-Gomez, 1991). Therefore, selection of appropriate kinetic and temperature model structures is important.

2.3. Modeling temperature sensitivity

Modeling temperature sensitivity is required to provide dynamic information on how the states of the anaerobic treatment process respond to temperature fluctuations. This information is useful in identifying time intervals where the AD process is most sensitive to such fluctuations or where temperature control of the digester is more or less important. For instance, if the sensitivity of methanogenic archae to temperature is close to zero in some time interval, changes in the value of temperature at that time interval would have little impact on biogas production. This information has significant economic importance because instead of heating the digester throughout the entire process (which is energy consuming), intermittent heating can be applied where the system is only heated at times were the states are most sensitive.

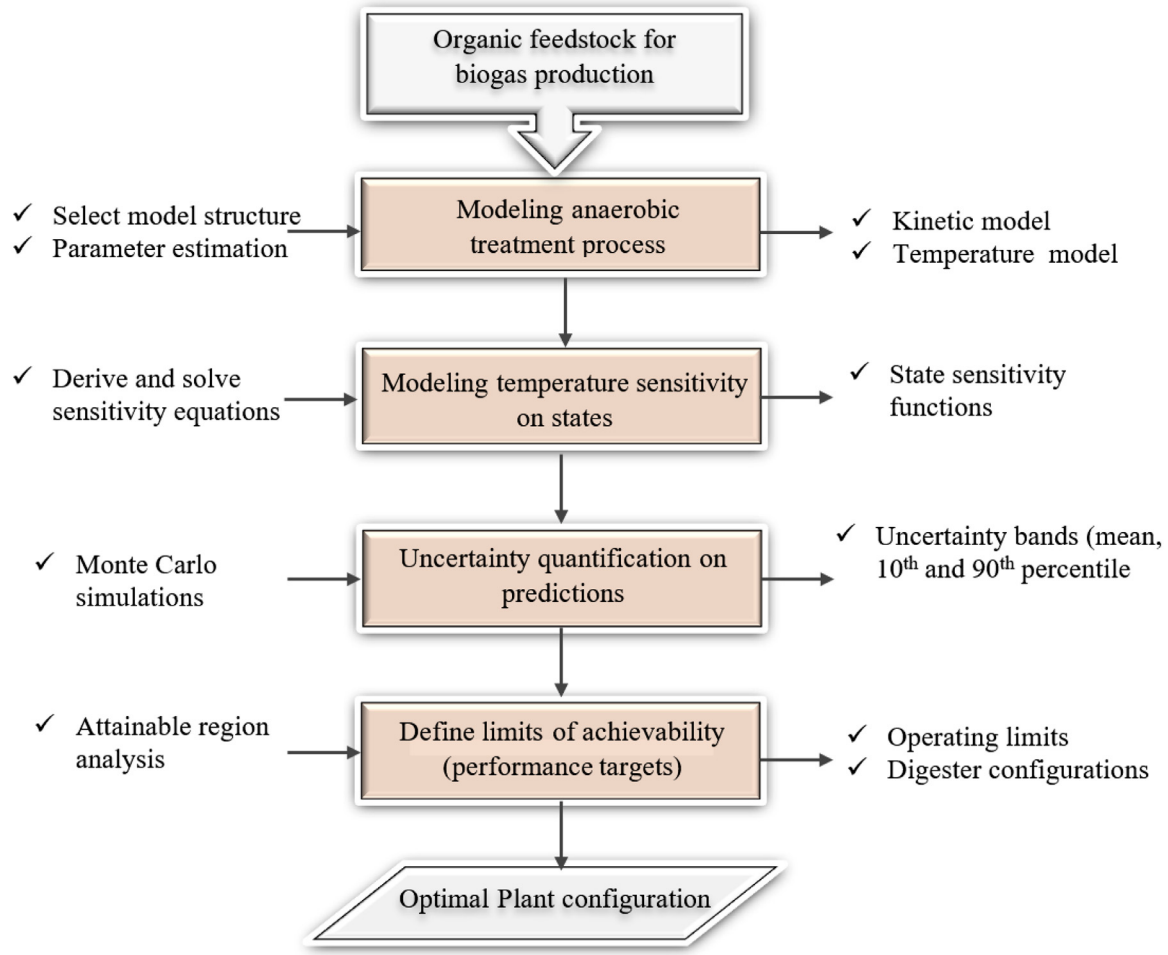

Fig. 1. Methodological work flow of the study.

2.4. Uncertainty quantification on prediction outputs

The uncertainty associated with the anaerobic treatment process arises from temperature fluctuations mainly due to seasonal variations, day–night patterns as well as specific spikes or drops events. The propagation of this uncertainty as well as calculation of uncertainty bounds (10th, percentile, mean and 90th percentile) on the model states was done using the Monte Carlo simulation method. This procedure is highly dependent on the temperature uncertainty range (known as variance metric of input).This variance metrics was obtained by measuring the ambient temperature over a two month period and using the data to fit a probability distribution from where the temperature was sampled during every iteration of the Monte Carlo procedure.

2.5. Maximum design and performance targets

For a given organic substrate and its concentration, the attainable region is the convex hull of the set of points achievable considering mixing and reaction (biodegradation) as the only fundamental processes occurring in the anaerobic digester. This defines the limits of achievability (performance targets of the process) and the boundary or the AR can be interpreted into digester configurations. It should be noted that if mixing and biodegradation are the only fundamental processes occurring in the digester, there is no need to devise new or perhaps novel digesters (other than the fundamental PFR and CSTR configurations) that can serve to expand the operating limits of the system (Ming et al., 2016). By expanding the performance targets, the authors mean achieving states that were initially not achievable considering mixing and biodegradation. Therefore, we call this point the maximum design and performance target.

3. Theoretical developments

The theoretical developments is divided into two main sections: the first section (Section 3.1) presents the kinetic and temperature dependence models of the anaerobic treatment process while the section (Section 3.2) presents the use of attainable region analysis to define the maximum design and performance targets of the AD process

3.1. Model of anaerobic biogas reactor

3.1.1. Kinetic model

The simplified dynamic model for anaerobic digestion of animal manure, which has been presented in our previous study (Abunde Neba et al., 2019c) for modeling configurations of anaerobic digesters using attainable regions was adopted in the current work. Fig. 2 presents a summary of the model scheme, clearly outlining the model inputs (temperature, organic load, retention time, waste and biomass characteristics) model outputs (volatile solids reduction and volumetric methane productivity), kinetic constants as well as state variables. This model is advantageous because the geometric calculations involved in attainable region analysis are relatively complex and it is required to have a simplified model

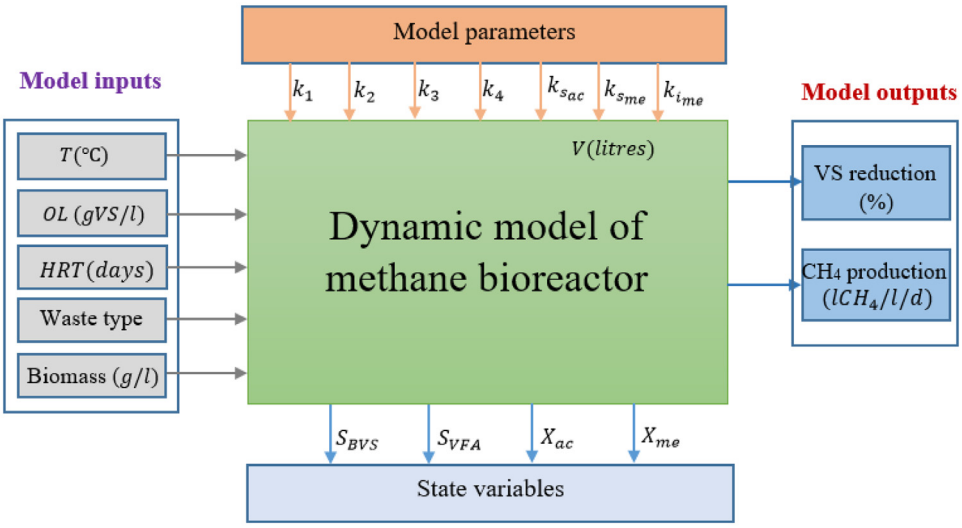

Fig. 2. Model of methane bioreactor showing inputs, outputs, parameters and state variables (Abunde Neba et al., 2019c).

(without compromise for process information) in order to make the problem more tractable.

The model considers four state variables, which include: Biodegradable Volatile Solids (BVS); Volatile Fatty Acids (VFA); acidogenic bacteria (X_{ac}) and methanogenic bacteria (X_{me}). The rate expressions for the four states are respectively presented by Eqs. (2) to (5).

$$\frac{dS_{BVS}}{dt} = r_{BVS} = -k_1 \mu_{ac} X_{ac} \tag{2}$$

$$\frac{dS_{VFA}}{dt} = r_{VFA} = \ k_2 \mu_{ac} X_{ac} - k_3 \mu_{me} X_{me} \tag{3}$$

$$\frac{dX_{ac}}{dt} = r_{ac} = \mu_{ac} X_{ac} \tag{4}$$

$$\frac{dX_{me}}{dt} = r_{me} = \ \mu_{me} X_{me} \tag{5}$$

The model assumes the specific death rates of both microbial populations are negligible compared to their specific growth rates. The specific growth rate of acidogenic bacteria is modeled using the Monod equation, Eq. (6) while an uncompetitive inhibition term is added to that of methanogenic bacteria, Eq. (7) to account for volatile acid inhibition during reactor upset or failure.

$$\mu_{ac} = \mu_{m_{ac}} \frac{S_{BVS}}{K_{s_{ac}} + S_{BVS}} \tag{6}$$

$$\mu_{me} = \mu_{m_{me}} \frac{S_{VFA}}{K_{s_{me}} + S_{VFA}\left(1 + \frac{S_{VFA}}{K_{i_{me}}}\right)} \tag{7}$$

The percentage volatile solids reduction and the volumetric methane productivity (model outputs) are calculated as presented in Abunde et al. (Abunde Neba et al., 2019c). The following parameters $k = [k_1,\ k_2,\ k_3,\ \vartheta,\ \gamma_s]$ are to be estimated while the values of all other parameters particularly $K_{s_{ac}},\ K_{s_{me}}$ and $K_{i_{me}}$ are maintained as in the original Hill model. The parameter estimation consisted of iteratively searching for parameter values that minimizes the squared error between the outputs predicted by the parameterized model and observed experimentally, Eq. (8).

$$\min_k \varepsilon(x,k) = \sum \left(\gamma_{CH_4}(k) - \gamma^e_{CH_4}\right)^2 + (VSR(k) - VSR^e)^2 \tag{8}$$

For this purpose, the Matlab optimization routine, *fmincon* was used, where the dynamic methane bioreactor model integrated numerically using the Runge-Kutta 4–5th order method implemented by the Matlab *ode45* routine. Table 1 presents the parameter estimates as well as model identification error computed for anaerobic digestion of diary manure. The calculated experimental values of model outputs, volatile solids reduction and volumetric methane productivity are 58.62% and 22.95 respectively while the model predicted values obtained are 58.60% and 22.91.

The biodegradability and acidity constants are unique to each type of waste Hill, 1983) and therefore serve to characterize the waste type being digested. For this study, respective values of 0.40 and 0.05 were used for the biodegradability and acidity constants. The effect of both constants on the initial concentration of states is modeled by Eqs. (9) and ((10).

$$S_{BVS_0} = B_0 (VS)_0 \tag{9}$$

$$S_{VFA_0} = A_f S_{BVS_0} \tag{10}$$

Characterizing the raw waste by using B_o and A_f simplifies the model since the effects of other parameters such as cation concentration, alkalinity, ammonia dissolved carbon dioxide are intrinsically part of B_o and A_f.

3.1.2. Temperature model

The effect of the temperature on the anaerobic treatment process has been modelled using the Ratkowsky expanded square root model, Eq. (11) (Ratkowsky et al., 1983). The advantage of this model is that it can describe the temperature influence over the entire biokinetic range of the anaerobic digestion process as opposed to the Arrhenius model, which only reproduces the increasing part of temperature dependence. The maximum growth rates of acid-forming bacteria ($\mu_{m_{ac}}$) and methane forming archae ($\mu_{m_{me}}$) are functions of the digestion temperature and this dependence was modeled as shown in Eq. (11)

$$\mu_{m_{ac}}(T) = \mu_{m_{me}}(T) = [B\ (T - T_{\min})]^2 \{1 - exp[C\ (T - T_{\max})]\}^2 \tag{11}$$

$$T_{\min} < T < T_{\max}$$

$T_{\min}$ and $T_{\max}$ are respectively the maximum and minimum temperatures at which the growth rate is zero while the constants

Table 1
Estimated kinetic coefficients and model identification error.

Parameter	k_1	k_2	k_3	ϑ	γ_s	K_{sac}	K_{me}	K_{ime}	Model error (ε)
Value	1.096	0.096	5.351	0.519	0.503	9.0	2.0	6.0	0.0435

B ($^\circ C^{-1}\ h^{-0.5}$) and C ($^\circ C^{-1}$) are known as Ratkowsky parameters, which are normally estimated from test data to reflect the process being modelled.

The determination of the Ratkowsky parameters (B and C) as well as $T_{\min}$ and $T_{\max}$ was made in our previous study by fitting the Chen and Hashimoto curve, cited by Hill (Hill, 1983) for temperature dependence on growth rate to the Ratkowsky expanded square root model. The parameters obtained were 0.02, 0.05, 4.22 and 79.96 respectively for $B, C, T_{\min}$ *and* $T_{\max}$ respectively.

3.2. Defining maximum design and performance targets

3.2.1. Temperature sensitivity modeling

Modeling temperature sensitivity consist of analyzing the sensitivity of the model states to the temperature. Given the kinetic and temperature model for the anaerobic digestion process, the following section illustrates how to model the temperature sensitivity on the anaerobic digester. Since we do not have an explicit solution to the complete process model, the absolute sensitivities must be computed using the sensitivity equations. For an n-dimensional system given by Eq. (12)

$$\dot{Y} = f(t, Y; \beta,\ T), \quad Y(0) = Y_0 \tag{12}$$

With $Y \in \mathbb{R}^n$, state variable, $\beta \in \mathbb{R}^p$ the model parameters, $T \in \mathbb{R}$ the temperature and Y_0 the initial condition, the vector of temperature sensitivities $\partial Y/\partial T$ satisfy

$$\frac{d}{dt}\frac{\partial Y}{\partial T} = \frac{\partial F}{\partial Y}\frac{\partial Y}{\partial T} + \frac{\partial F}{\partial T} \tag{13}$$

With initial conditions

$$\frac{\partial Y(0)}{\partial T} = 0_{n\times 1} \tag{14}$$

$\partial Y/\partial T$ is the change of states with respect to temperature. The sensitivity equations are coupled with the original model differential equations and solved to obtain the temperature sensitivities for the necessary time points. The resulting matrix of absolute sensitivities at time point t $S_a(t) = \partial Y/\partial T$ will be of the form shown by Eq. (15).

$$S_a(t) = \begin{bmatrix} S_{1,t_1} & S_{2,t_1} & S_{3,t_1} & S_{4,t_1} \\ S_{1,t_2} & S_{2,t_2} & S_{3,t_2} & S_{4,t_1} \\ \vdots & \vdots & \vdots & \vdots \\ S_{1,t_n} & S_{2,t_n} & S_{3,t_n} & S_{4,t_n} \end{bmatrix} \tag{15}$$

3.2.2. Propagation of temperature uncertainty

The global optimization technique of attainable regions is based on a geometric representation (or convex hull) of model states (or set of points) that are achievable by the system. Any factor that influences the states being output by the digester will therefore influence the operating limits of the system, which is defined by the attainable region. The propagation of temperature uncertainty on to the model states was done using the Monte Carlo simulation procedure, which involves three steps: (1) specifying temperature uncertainty range, usually in the form of a statistical distribution (2) sampling a defined number of values form the distribution in which case we used 1000 and (3) propagating the sampled input uncertainty on to the model states. The temperature was sampled randomly from a uniform distribution with minimum and maximum values of 20$^\circ C$ and 60$^\circ C$ respectively. The uncertainty bands, 10th percentile, mean and 90th percentile were used to quantify the degree of uncertainty for each of the predicted model states resulting from temperature uncertainty. These important levels within the uncertainty range will be used to propagate the states uncertainty onto the boundary of the attainable regions in order to define the self-optimizing attainable regions (see Section 4.3).

3.2.3. Attainable region analysis

After defining the process model and calculating the output (model states) uncertainty bands resulting from input (temperature) uncertainty, attainable region analysis can now be used to define the performance targets of the anaerobic treatment process. The following section outlines the methodological framework for AR construction, its application for process synthesis as well as for defining the self-optimizing operating limits under non-isothermal conditions. The framework involves five main steps:

Step 1: Preparation

This involves definition of the reaction kinetics, AR dimension, state variables (those used to represent the AR) as well as the feed point and temperature values that correspond to the mean, 10th and 90th percentile of the state uncertainty bands. A stoichiometric scheme of the bioreaction occurring in the methane bioreactor consist of two main reactions catalyzed by acid-forming bacteria, Eq. (16) and methane-forming bacteria Eq. (17)

$$k_1 S_{BVS} \xrightarrow{r_{X_{ac}}} X_{ac} + k_2 S_{VFA} \tag{16}$$

$$k_3 S_{VFA} \xrightarrow{r_{X_{me}}} X_{me} + k_4 CH_4 \tag{17}$$

Letting rows 1–5 correspond to S_{BVS}, X_{ac}, S_{VFA}, X_{me} and CH_4 respectively, the stoichiometric coefficient matrix A is therefore a 5×2 matrix, given by Eq. (18)

$$A = \begin{bmatrix} -k_1 & 0 \\ 1 & 0 \\ k_2 & -k_3 \\ 0 & 1 \\ 0 & k_4 \end{bmatrix} \tag{18}$$

Since there are two independent reactions participating in the system ($Rank(A) = 2$), we expect the set of points generated by the anaerobic treatment process to reside in a two-dimensional subspace in $\mathbb{R}^5$. As all model outputs are functions of volatile fatty acids and concentration of methanogenic bacteria, it is sensible to generate the AR in ($S_{VFA} - X_{me}$) space, which provides information required to maximize gas production and volatile solids reduction.

The number of dimensions in which the AR must be constructed was reduced using the concept of yield coefficients, which has been used previously to reduce the number of dimensions during AR analysis (Scott et al., 2013).

This implies that the concentrations of BVS and acidogenic bacteria can be expressed as a function of VFA and methanogenic bacteria concentrations as in Eqs. (19) and (201).

$$X_{ac} = X_{ac_0} + \frac{1}{k_2}\left[S_{VFA} - S_{VFA_0} + k_3(X_{me} - X_{me_0})\right] \tag{19}$$

$$S_{BVS} = S_{BVS_0} - \frac{k_1}{k_2}\left[S_{VFA} - S_{VFA_0} + k_3(X_{me} - X_{me_0})\right] \tag{20}$$

The ability to calculate X_{ac} and S_{BVS} as a function of X_{me} and S_{VFA} allow us to also express the rate and concentration vectors of

X_{me} and S_{VFA} exclusively. In other words, for each X_{me} and S_{VFA} in the $(S_{VFA} - X_{me})$ space we can calculate a rate vector that uniquely determines the CSTR locus and PFR trajectory from a specified organic load.

Step 2: AR construction

For each of the three temperature values (the temperature values that correspond to the mean, 10th and 90th percentile of the state uncertainty bands), the AR is generated using a combination of PFR, CSTR and mixing. This is the most difficult and time-consuming step but also provides the most valuable information about the operating limits of the system. AR construction typically begins by determining the PFR trajectory and CSTR locus from the feed. The PFR trajectory is the set of points generated by solving the steady state model of a PFR reactor (a set of ordinary differential equations) while the CSTR locus is the set of points generated by solving the CSTR model (a set of nonlinear equations). The convex hull for the set of all possible points generated by all possible combinations of PFR, CSTR and mixing defines the attainable region. The CSTR equations are solved using Newton method, implemented by the Matlab routine 'fsolve' while the PFR equations are solved using the Runge-Kutta 4th to 5th order algorithm implemented by the Matlab *ode45* routine for solving non-stiff differential equations. The convex hall of the entire set of geometric points is obtained by using the Matlab '*convhull*' routine, which implements the Qhull algorithm (Mathworks, Natick NA).

Step 3: Boundary Interpretation

This step involves interpretation of the AR boundary into reactor structures, based on the fundamental characteristics of the AR boundary. The boundary of the AR is composed of reaction and mixing surfaces only. Reaction surfaces are always convex and the points that form convex sections of the AR boundary arise from effluent concentrations specifically from PFR trajectories. For a two-dimensional system, points on the AR boundary that initiate these convex PFR trajectories arise from specialized CSTRs. This information is used to determine digester configurations required to achieve the points located within and on the boundary of the attainable region.

Step 4: Define self-optimizing operating limits

After constructing the attainable regions that correspond to the mean, 10th and 90th percentile of the state uncertainty bands, the self-optimizing operating limits of the system can be obtained. This is done by overlaying each of the three ARs onto one another and determining the region of intersection between all the regions. The intersection region, though usually smaller than each of the individual ARs, will always be attainable in spite of the variations in temperature within the predefined uncertainty range. Since the entire boundary of the individual ARs have already been interpreted in terms of reactor structures (step 3), the particular reactor required to achieve points on the self-optimizing AR is known.

4. Results and discussion

4.1. Temperature sensitivity analysis

As earlier pointed out in the introduction to this article, the goal has been to define the performance targets of biogas plants operated under non-isothermal conditions (plants where temperature is not controlled). This shows a need to be explicit about exactly what is meant by the word performance targets for non-isothermal biogas plants, which implies what is achievable albeit all possible variations in temperature. Figs. 3 and 4 compares the results obtained from analysing the sensitivities of the four process states to the operating temperature of the biogas digester.

From the Figures, it can be seen that within the 28 days of anaerobic digestion, the greatest influence of temperature on the process states is during start-up (first five days of operation). However, at this stage, a conclusion cannot be made with certainty, as we don't know if this effect could be due to defined value of temeprature ($35^{\circ}C$) used to obtain the sensitivity functions. Recall from Section 3.1.2 that the temperature dependence of the anaerobic treatment process has been modelled using the Ratkowsky expanded square root model, Eq. (11). Because there is no explicit solution for the kinetic model (system of ordinary differential equations) of the anaerobic treatment process, the sensitivity equations are coupled with the original model differential equations and solved to obtain the temperature sensitivities for the necessary time points. This entail defining a value for temperature in the Ratkowsky expanded square root model before the coupled system of equations can be solved. In order to ensure the obtained sensitivity effects are not depended upon the defined value of temperature, the Monte Carlo procedure was applied to visualize the effect of inputs (different defined temperatures between 20 and $60^{\circ}C$) on the outputs (behavior of the sensitivity functions). Figure four presents the overall behaviors of the sensitivity function for 1000 Monte Carlo simulations. Notice that despite variations in the defined value of the temperature, the sensitivity of the process states to temperature is still very significant only at the startup of the anaerobic treatment process.

Taken together, the observations from Figs. 3 to 5 suggest that temperature has a significant effect during start-up of the anaerobic treatment process. Interestingly, this correlation is because during the early stages of anaerobic digestion, the anaerobic microorganisms are still trying to acclimatize to the conditions of the waste. The acclimatization of anaerobic microorganisms is influenced by temperature and other factors such as waste characteristics, inoculum activity, pH, loading rate, retention time and reactor configuration (Weiland and Rozzi, 1991; Ghangrekar et al., 1996). This study focuses on the interactions between temperature and reactor configuration as this accord with observations from other studies, investigating the effect of modifying the digester configurations to overcome the influence of temperature (Chong et al., 2012; Gaby et al., 2017).

4.2. Uncertainty quantification

Having discussed how sensitive the process states are to temperature, we now present the actual quantification of the overall effect of temperature on the process states. Fig. 6 presents the propagation of temperature uncertainty onto the model states, which has been quantified using the 10th percentile, mean as well as the 90th percentile. Observe that the uncertainty band (10th and 90th percentile) is widest within the first few days of operating the anaerobic treatment process, which further supports the high temperature influence during process start-up. It is important for readers to note that the uncertainty bands presented in Fig. 6 are dependent on the temperature uncertainty range (20 - $60^{\circ}C$) used for the Monte Carlo simulation.

The results are interpreted as follows: the larger the uncertainty band (difference between the 10th and 90th percentiles), the lower the model prediction quality. Accordingly, due to temperature uncertainty, the model prediction quality is low for all the four states within the first few days of operation. The attainable regions, which defines the limits of achievability of a process is based on the attainability of states and uncertainty in the states will therefore results in uncertainty in defining the operating limits of the system. Hence model uncertainty, resulting from temperature uncertainty reduces the reliability of using attainable regions for defining process performance targets. This is where the strength of this study comes into play where we quantify the model prediction uncertainty and incorporate its effect when defining the operating limits of the system (object of the next section).

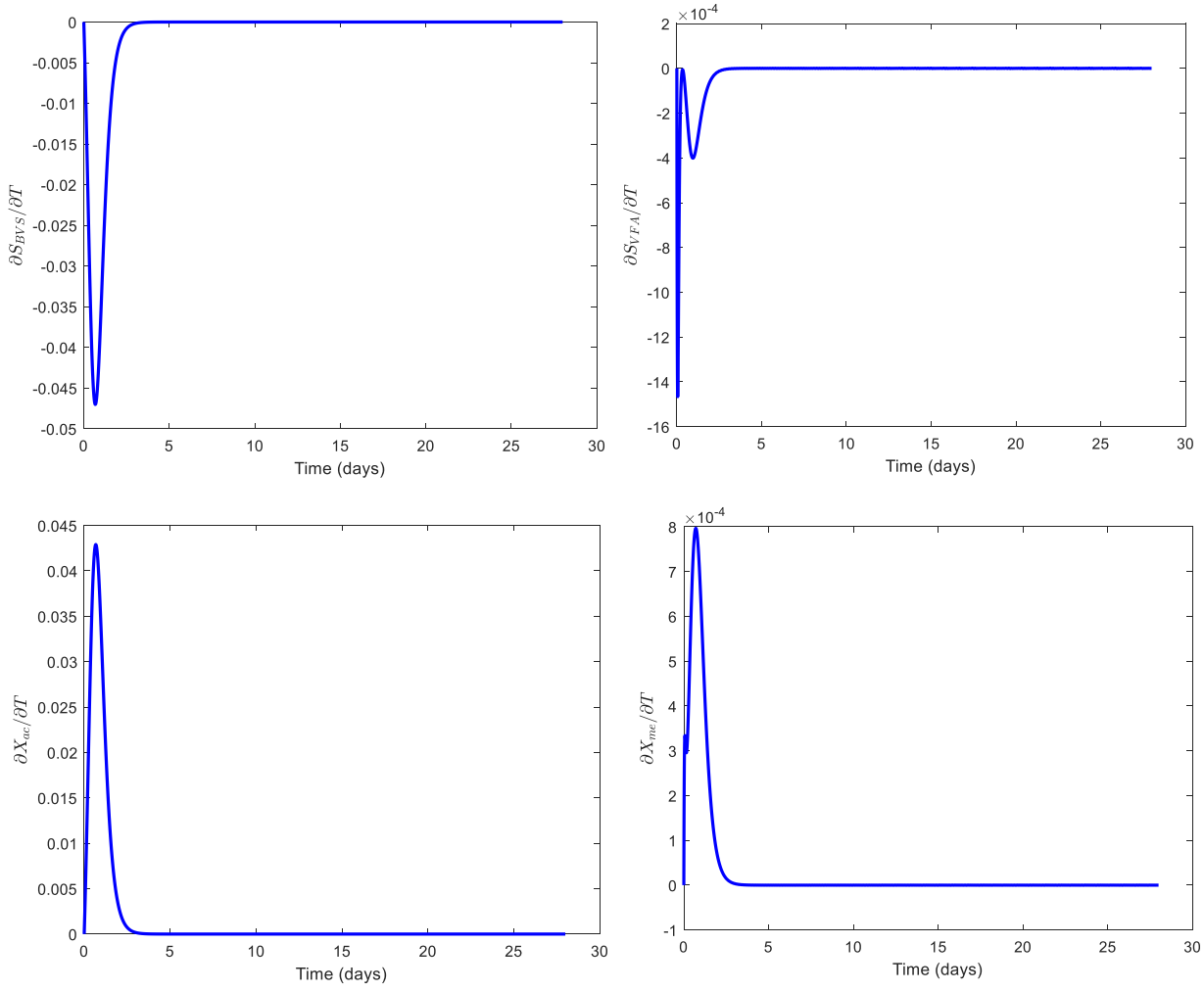

Fig. 3. Sensitivity functions of model states to temperature.

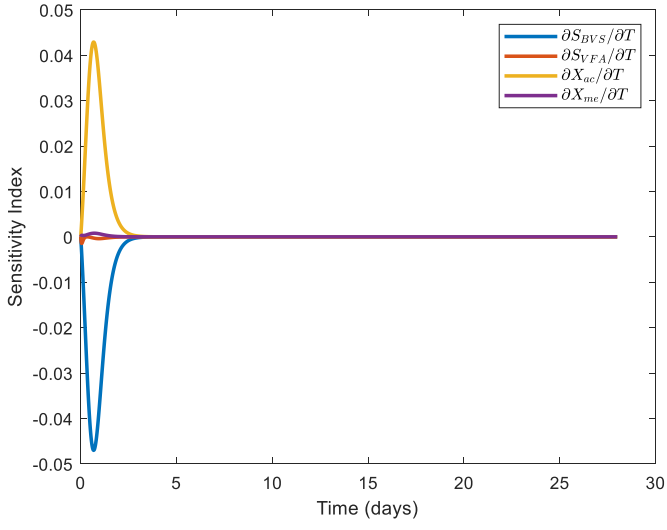

Fig. 4. Superposing sensitivity functions of model states to temperature.

4.3. Operating limits and optimal plant configurations

So far, this paper has illustrated the sensitivity of the model states to temperature and how uncertainty in temperature reduces the quality of model prediction. The following section will discuss how to correct for model prediction uncertainty when using the model to define the operating limits of the anaerobic treatment process. The attainable region is defined as the convex hull for the set of states achievable from different combinations of PFR, CSTR and mixing. Hence in order to factor in temperature uncertainty, we make use of the state's uncertainty bands (mean, 10th and 90th percentile) that have been computed in Section 4.2. This is done by constructing the attainable regions using the temperature values that correspond to uncertainty bands and determining the region of intersection between the three individual regions. The temperature values the gave the mean, 10th and 90th percentile of the state prediction was respectively 31.60, 20.00 and 52.40°C.

Figs. 7 to 9 present the attainable regions constructed using the temperatures that correspond to the 10th percentile, mean and 90th percentile state uncertainty bands respectively. The boundaries of the attainable regions have been interpreted into digester configurations, which can be used to attain the different operating limits defined by the regions. The boundary of the attainable region represents the smallest subset of points that can generate all other points achievable by the system using possible combinations of fundamental reactor types and mixing (Ming et al., 2016). This smallest subset of points is referred to as the convex hull, which for a two-dimensional AR, is interpreted as the smallest polygon enclosed by planar facets where by all elements lie on or within the polygon (Asiedu et al., 2015). The authors now illustrate the in-

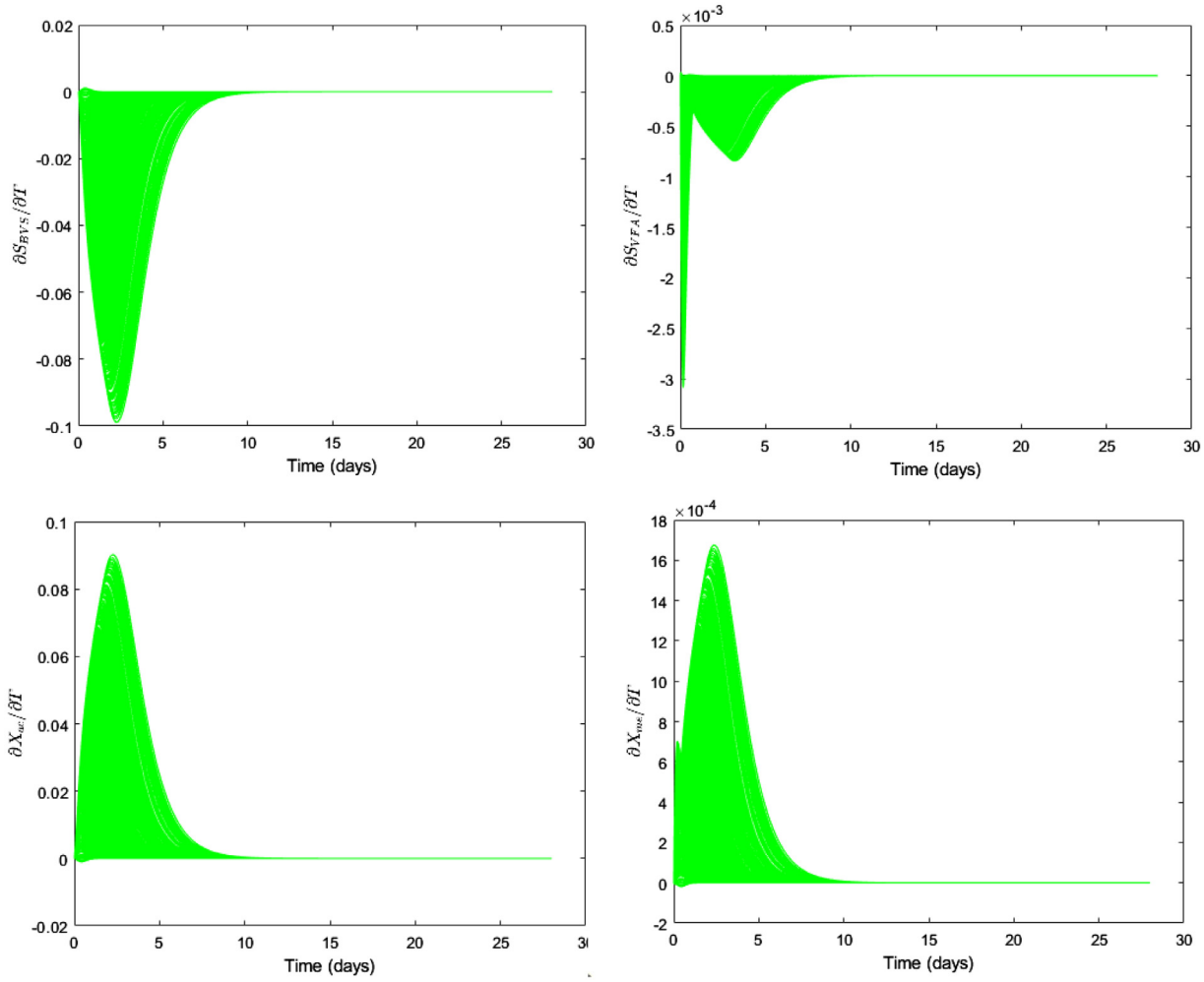

Fig. 5. Influence of temperature on process states for 1000 Monte Carlo Simulations.

terpretation of the AR boundary into reactor structures using Fig. 7. On Fig. 7, the point A is the feed, while the line AC and region defined by points ABC is the AR. The convex segment AB is known as the PFR trajectory while segment A to D is called CSTR locus. The curves represented by E (moving from CSTR locus to point C) are PFR trajectories obtained using concentrations on the CSTR locus as feed conditions. The point C is therefore obtained by running a CSTR from the feed (point A) followed by a PFR from CSTR effluent. As mentioned in Section 3.2.3 (step 3), the boundary of the AR is composed of reaction and mixing surfaces only. Mixing surfaces are always straight lines while reaction surfaces are always convex and the points that form convex sections of the AR boundary arise from effluent concentrations specifically from PFR trajectories. The line AC is therefore a mixing line while the curve AB is a reaction surface. Concentrations that lie along the mixing line AC (C_{AC}) can be obtained by mixing points A and C, and generally follows the lever-arm rule, Eq. (21). The reactor structure required to achieve points on the mixing line AC is therefore given by a CSTR+PFR (point C) with a bypass from point A.

$$C_{AC} = \alpha C_A + (1-\alpha)C_C, \qquad 0 \le \alpha \le 1 \tag{21}$$

Where α is known as the mixing ratio. Similar reactor interpretations were made for the other substrates as presented in Figs. 8 and 9. It is not the intention of this article to go into detailed explanation of the geometry involved in interpreting the AR boundary into the digester configurations, interested readers can consult the previously cited papers.

Three interesting remarks can be made from the Figs. 7 to 9. (1) An increase in temperature of the digester increases the operating limits of the system. The operating limit is defined by the area of the convex hull, which is computed as of 1.53×10^{-4}, 4.95×10^{-4} and 6.32×10^{-4} $(g/L)^2$ for the 10th percentile, mean and 90th percentile respectively. This because an increase in temperature (within a certain range) generally increases the rate of the anerobic digestion and hence more states will be output by the systems operating at higher temperatures. (2) Using a multistage digester configuration as opposed to a single digester increases the operating limits of the anerobic treatment process. Points that can be achieved by the system are only those located within the attainable region. For all the temperatures higher concentrations of methanogenic archaea can be obtained for higher concentrations of volatile fatty acids only using a multistage digester configuration consisting of a CSTR followed by a PFR and by pass from feed. This is because multistage digester configurations are optimized each step (acid formation and methane production steps) of the anaerobic treatment process (EPA, 2006). (3) A change in the operating temperature does not affect the geometry of the attainable region boundary but only the limits of achievability, area of the convex hull (as explained in the first remark above). This is quite interesting because the geometry of the attainable region is unique for a given kinetics and feed point and not for temperature (Hildebrandt and Glasser, 1990; Hildebrandt et al., 1990).

The results all put together imply that temperature and digester configuration have a significant effect on the operating limits of

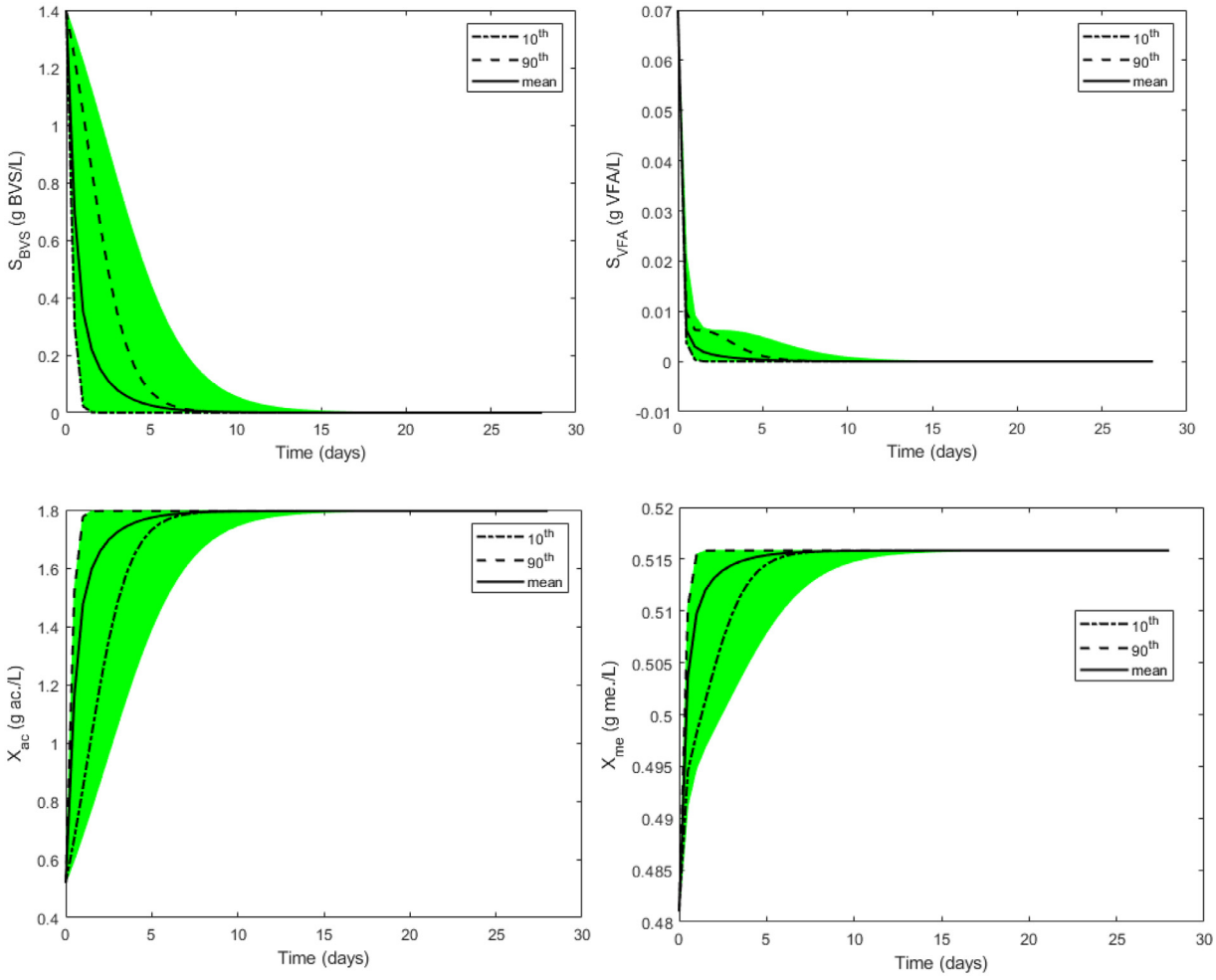

Fig. 6. State uncertainty bands obtained from 1000 Monte-Carlo Simulations.

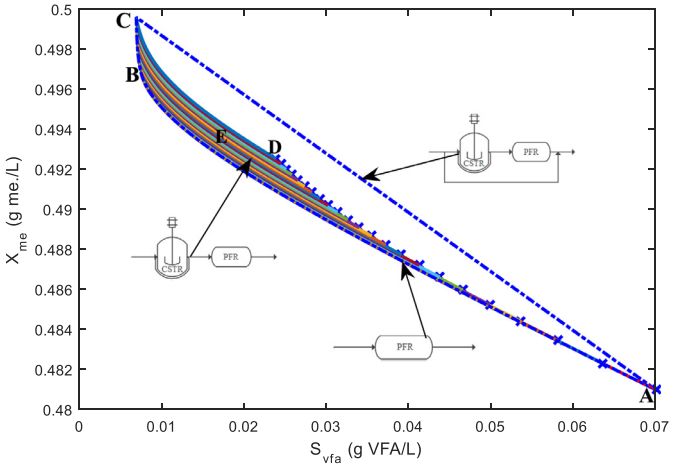

Fig. 7. Attainable region (operating limits) for 10th percentile state prediction.

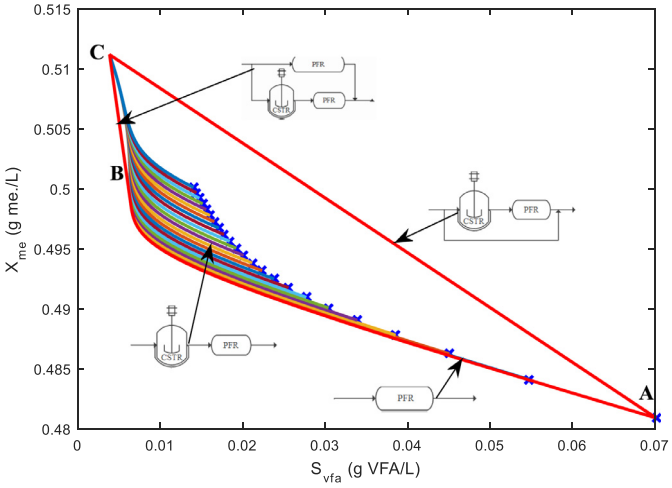

Fig. 8. Attainable region (operating limits) for mean state prediction.

the anaerobic treatment process and hence modifying the temperature or reactor configuration would affect the performance of the anaerobic treatment process. This accords the findings of previous studies reporting that modifying the reactor configuration and or temperature influences the performance of the anaerobic treatment process. A practical example is the use of a multistage dieter consisting of a UASB (a kind of plug flow digester) and a CSTR to improve performance targets of anaerobic digestion under variable temperature conditions (Lettinga and Hulshoff Pol, 1991; Mahmoud et al., 2004).

Fig. 10 present the intersection of the three regions to define the self-optimizing attainable region of the anaerobic treatment process. Notice that the intersection region (region bounded by

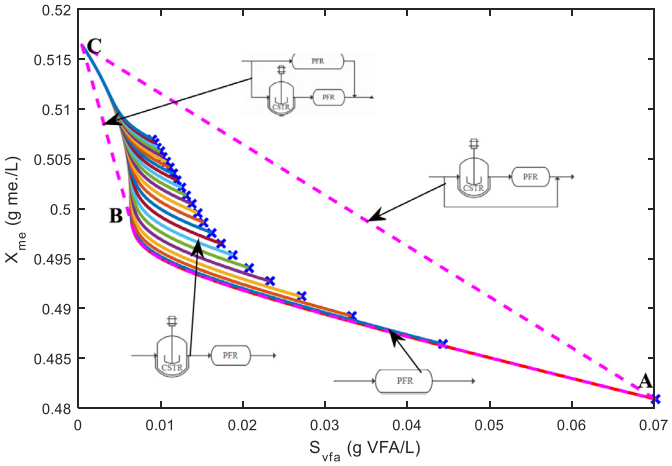

Fig. 9. Attainable region (operating limits) for 90th percentile state prediction.

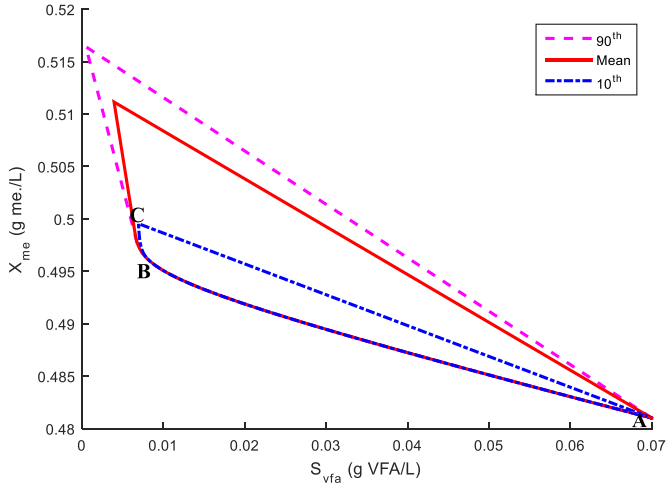

Fig. 10. Superposition of attainable regions showing the self-optimizing attainable regions.

ABC) corresponds to the 10th percentile attainable region. This is an interesting feature that the authors notice when defining self-optimizing attainable regions using temperature uncertainty (as opposed to kinetic uncertainty). An explanation for this observation is that the states that are achievable at lower temperatures will also be achieved at higher temperatures but not all states that are achievable at higher temperatures can be achieved at lower temperatures. Put it in another way, since the rate of digestion increases with temperature (of course within a given range), all other things being equal, a given quantity of biogas produced by a plant operating at a lower temperature can also be produced by a plant operating a higher temperature. The difference is that the plant operating at higher temperature will produce more biogas in addition to the one that is produced by the plant operating at lower temperature. However, generally, the self-optimizing attainable region is generally smaller than the true AR because self-optimality implies an acceptable loss in operating limits. It is necessary here to re-define exactly what is meant by self-optimizing attainable regions. Unlike the attainable region, which represents the set of all possible states that is achievable by the system for a defined temperature, kinetics and organic load (feed point), the self-optimizing attainable region represents the set of all possible states attainable by the system even in cases of temperature uncertainty. The size of the self-optimizing attainable region is conditional to the uncertainty domain (20 – 60°C) defined for temperature during the propagation of temperature uncertainty using the Monte Carlo simulation procedure. The larger the domain of uncertainty, the smaller the area of the self-optimizing AR and vice versa and hence incorporating temperature uncertainty reduces the operating limits of system. However, other than defining a very large operating limit, which will be achieved some of the times (for fixed temperature values), we define a smaller limit which will be achieved all of the times (despite variations in temperature).

The findings from this study are therefore highly important in making economic feasibility decisions about the performance of biogas plants especially in cases where accuracy is very necessary. This is a key motivation for renewable energy investors as it is better to making investment decisions for biogas plants using worse case performance target. This is because if evaluations indicate that the investment is profitable, then even better profitability indices will be obtained during real-time operation if the environmental conditions (mainly temperature) favor the kinetics of the anaerobic treatment process. Even in cases where the environmental conditions are unfavorable, we are sure to still be profitable since investment decisions have been made using a worse-case scenario. The results of this study are therefore high applicable to countries where biogas plants are operated either under isothermal or non-isothermal conditions.

Summarily, the results, which show that the operating limits, defined by the AR differs for each operating temperature, provides the following noteworthy contributions of practical relevance: For plants operated under isothermal conditions, the study provides a framework for obtaining unique optimal digester configurations, which are specific to the digestion temperature under consideration (psychrophilic, mesophilic or thermophilic ranges). For the case of non-isothermal plants, the study proposes a self-optimizing approach to define performance targets, which are optimal for all temperatures within a defined boundary. This study though preliminary presents a breakthrough in extending the use of digester networks to solve more operational challenges as such systems can optimize every step in the anaerobic treatment process. For an already existing anaerobic digestion plant, the AR concept shows the proximity of the existing system in relation to the absolute best performance, which is important in deciding whether or not to invest resources to optimize the plant.

It is interesting to compare the approach to digester network synthesis presented in this study with that presented in previous studies. The conventional superstructure optimization technique for digester network synthesis Pontes and Pinto, 2009) suffers from multiple solutions (or local optimum) because it involves a very large reactor superstructure and provides no systematic approach for answering the following three questions about the optimal digester network: ((1) what number of individual digesters should be in an optimal network. (2) Should by-pass or recycle streams be included, if yes (3) where in the network should they be positioned. The uniqueness and strength of the AR approach is that it provides the absolute best performance (totality of achievable states) for all possible digester configurations (even those that have not yet been devised).

As mentioned in the introduction, the other papers on the AR concept work for isothermal biogas plants. This study is highly novel by introducing a self-optimizing concept for non-isothermal conditions through the propagation of temperature uncertainty onto the AR boundary to define the self-optimizing attainable regions. The idea of self-optimizing attainable regions first introduced in a recent paper published by the authors (Abunde Neba et al., 2020) is that instead of having an optimal performance target, which can only be achieved some of the times (due to temperature fluctuations), it is better to define a near optimal operating target, which is achievable all of the times. The current paper has extended the concept of self-optimizing attainable

regions from kinetic uncertainty to temperature uncertainty, which is a very important parameter for practical operation of anaerobic digestion.

5. Conclusion

The present study was designed to lay down a theoretical framework for defining self-optimizing operating limits for biogas plants operated under non-isothermal conditions. This study has shown that temperature and digester configuration have a significant effect on the operating limits of biogas plants and hence modifying the temperature or reactor configuration would affect the performance of the anaerobic treatment process. The second and major finding is that the larger the variations of operating temperature, the smaller the self-optimizing operating limits of the plant and vice versa. The findings from this study make an interesting contribution to the current literature on applying attainable regions for synthesis and optimization of biogas plants as the study is first of its kind illustrating how to factor in the uncertainty in operating conditions during attainable region analyses.

The findings from this study though preliminary, suggest that other than defining a very large operating limit, which will be achieved some of the times (for fixed temperature values), it is possible to define a smaller limit which will be achieved all the times (despite variations in temperature). More research is needed to extend the concept of self-optimizing attainable regions in the field of anaerobic digestion. Further investigation is needed to assess the effects of other sources of operational uncertainty (such as substrate characteristics, presence of inhibitions) on the operating limits of biogas plants.

Funding

This work was supported by EnPe-NORAD under the project Upgrading Education and Research Capacity in Renewable Energy Technologies (UPERC-RET).

Author statement

F. Abunde Neba: Conceptualized the work, developed the methodological framework, conducted theoretical developments, numerical computations, analyzed the results as well wrote, reviewed and edited the paper.

Hoese Michel Tornyeviadzi: He helped with conceptualization and formal analysis of the mathematical models.

Nana Y. Asiedu: He helped with conceptualization as well review and interpretation of results.

Ahmad Addo: He helped with interpretation of results as well as review and editing of the paper.

John Morken: He helped with scientific resources as well as review and interpretation of the results.

Stein W. Østerhus: He helped with scientific resources, interpretation of results as well as review and editing.

Razak Seidu: He acquired the funding leading to the research. He also helped with scientific resources, interpretation of results as well review and editing of the paper.

Declaration of Competing Interest

The authors declare that they have no known competing financial interests or personal relationships that could have appeared to influence the work reported in this paper.

Acknowledgments

Our team expresses gratitude to the following institutions; The Brew-Hammond Energy centre, KNUST Ghana, The Water and Environmental Engineering Group, NTNU Ålesund and the Abunde Sustainable Engineering Group (AbundeSEG) for its immense technical support.

References

Abunde Neba, F., Asiedu, N.Y., Addo, A., Morken, J., Østerhus, S.W., Seidu, R., 2019a. Biodigester rapid analysis and design system (B-RADeS): a candidate attainable region-based simulator for the synthesis of biogas reactor structures. Comput. Chem. Eng. Accepted Manuscript.

Abunde Neba, F., Asiedu, N.Y., Addo, A., Morken, J., Østerhus, S.W., Seidu, R., 2019b. Simulation of two-dimensional attainable regions and its application to model digester structures for maximum stability of anaerobic treatment process. Water Res., 114891.

Abunde Neba, F., Asiedu, N.Y., Addo, A., Morken, J., Østerhus, S.W., Seidu, R., 2019c. Use of attainable regions for synthesis and optimization of multistage anaerobic digesters. Appl. Energy 242, 334–350.

Abunde Neba, F., Asiedu, N.Y., Addo, A., Seidu, R., 2019d. Attainable regions and fuzzy multi-criteria decisions: modeling a novel configuration of methane bioreactor using experimental limits of operation. Bioresource Technol., 122273.

Abunde Neba, F., Tornyeviadzi, H.M., Østerhus, S.W., Seidu, R., 2020. Self-optimizing attainable regions of the anaerobic treatment process: modeling performance targets under kinetic uncertainty. Water Res. 171, 115377.

Akobi, C., Yeo, H., Hafez, H., Nakhla, G., 2016. Single-stage and two-stage anaerobic digestion of extruded lignocellulosic biomass. Appl. Energy 184, 548–559.

Asiedu, N., Hildebrandt, D., Glasser, D., 2015. Experimental simulation of three-dimensional attainable region for the synthesis of exothermic reversible reaction: ethyl acetate synthesis case study. Ind. Eng. Chem. Res. 54, 2619–2626.

Bandara, Wasala M.K.R.T.W., Kindaichi, T., Satoh, H., Sasakawa, M., Nakahara, Y., Takahashi, M., Okabe, S., 2012. Anaerobic treatment of municipal wastewater at ambient temperature: analysis of archaeal community structure and recovery of dissolved methane. Water Res. 46, 5756–5764.

Bustamante, M., Liao, W., 2017. A self-sustaining high-strength wastewater treatment system using solar-bio-hybrid power generation. Bioresour. Technol. 234, 415–423.

Chong, S., Sen, T.K., Kayaalp, A., Ang, H.M., 2012. The performance enhancements of upflow anaerobic sludge blanket (UASB) reactors for domestic sludge treatment – a state-of-the-art review. Water Res. 46, 3434–3470.

De Vrieze, J., Arends, J.B.A., Verbeeck, K., Gildemyn, S., Rabaey, K., 2018. Interfacing anaerobic digestion with (bio)electrochemical systems: potentials and challenges. Water Res. 146, 244–255.

Donoso-Bravo, A., Bandara, Wasala M.K.R.T.W., Satoh, H., Ruiz-Filippi, G., 2013. Explicit temperature-based model for anaerobic digestion: application in domestic wastewater treatment in a UASB reactor. Bioresour. Technol. 133, 437–442.

EPA, U.S.E.P.A., 2006. Biosolids Technology Fact Sheet, Multi-Stage Anaerobic Digestion. National Service Center or Environmental Publications (NSCEP).

Gaby, J.C., Zamanzadeh, M., Horn, S.J., 2017. The effect of temperature and retention time on methane production and microbial community composition in staged anaerobic digesters fed with food waste 10, 302.

Gausemeier, J., Frank, U., Schmidt, A., Steffen, D., 2006. Towards a design methodology for self-optimizing systems. In: Elmaraghy, H.A., Elmaraghy, W.H. (Eds.), Advances in Design. Springer London, London.

Ghangrekar, M.M., Asolekar, S.R., Ranganathan, K.R., Joshi, S.G., 1996. Experience with UASB reactor start-up under different operating conditions. Water Sci. Technol. 34, 421–428.

Henze, M., Van Loosdrecht, M.C.M., Ekama, G.A., Brdjanovic, D., 2008. Biological Wastewater Treatment. IWA Publishing.

Hildebrandt, D., Glasser, D., 1990. The attainable region and optimal reactor structures. Chem. Eng. Sci. 45, 2161–2168.

Hildebrandt, D., Glasser, D., Crowe, C.M., 1990. Geometry of the attainable region generated by reaction and mixing: with and without constraints. Ind. Eng. Chem. Res. 29, 49–58.

Hill, D.T., 1983. Simplified monod kinetics of methane fermentation of animal wastes. Agric. Wastes 5, 1–16.

Kafle, G.K., Chen, L., 2016. Comparison on batch anaerobic digestion of five different livestock manures and prediction of biochemical methane potential (BMP) using different statistical models. Waste Manag. 48, 492–502.

Kim, M.-.S., Kim, D.-.H., Yun, Y.-.M., 2017. Effect of operation temperature on anaerobic digestion of food waste: performance and microbial analysis. Fuel 209, 598–605.

Kuo, W.-.C., Lai, W.-.L., 2010. Treatment of kitchen waste using a mobile thermophilic anaerobic digestion system. Renew. Energy 35, 2335–2339.

Latif, M.A., Ahmad, A., Ghufran, R., Wahid, Z.A., 2012. Effect of temperature and organic loading rate on upflow anaerobic sludge blanket reactor and CH4 production by treating liquidized food waste. Environ. Prog. Sustain. Energy 31, 114–121.

Lettinga, G., Hulshoff Pol, L.W., 1991. UASB-process design for various types of wastewaters. Water Sci. Technol. 24, 87–107.

Li, C., Champagne, P., Anderson, B.C., 2013. Biogas production performance of mesophilic and thermophilic anaerobic co-digestion with fat, oil, and grease in semi-continuous flow digesters: effects of temperature, hydraulic retention time, and organic loading rate. Environ. Technol. 34, 2125–2133.

Lohani, S.P., Wang, S., Bergland, W.H., Khanal, S.N., Bakke, R., 2018. Modeling temperature effects in anaerobic digestion of domestic wastewater. Water-Energy Nexus 1, 56–60.

Mahmoud, N., Zeeman, G., Gijzen, H., Lettinga, G., 2004. Anaerobic sewage treatment in a one-stage UASB reactor and a combined UASB-Digester system. Water Res. 38, 2348–2358.
Ming, D., Glasser, D., Hildebrandt, D., 2013. Application of attainable region theory to batch reactors. Chem. Eng. Sci. 99, 203–214.
Ming, D., Glasser, D., Hildebrandt, D., Glasser, B., Metzer, M., 2016. Attainable Region Theory: An Introduction to Choosing an Optimal Reactor. John Wiley & Sons, Inc, Hoboken, New Jersey.
Pavlostathis, S.G., Giraldo-Gomez, E., 1991. Kinetics of anaerobic treatment: a critical review. Critic. Rev. Environ. Control 21, 411–490.
Permin, E., Bertelsmeier, F., Blum, M., Bützler, J., Haag, S., Kuz, S., Özdemir, D., Stemmler, S., Thombansen, U., Schmitt, R., Brecher, C., Schlick, C., Abel, D., Poprawe, R., Loosen, P., Schulz, W., Schuh, G., 2016. Self-optimizing production systems. Procedia CIRP 41, 417–422.
Pontes, R.F.F., Pinto, J.M., 2009. Optimal synthesis of anaerobic digester networks. Chem. Eng. J. 149, 389–405.
Ratkowsky, D.A., Lowry, R.K., Mcmeekin, T.A., Stokes, A.N., Chandler, R.E., 1983. Model for bacterial culture growth rate throughout the entire biokinetic temperature range. J. Bacteriol. 154, 1222–1226.
Saady, N.M.C., Massé, D.I., 2015. Impact of organic loading rate on the performance of psychrophilic dry anaerobic digestion of dairy manure and wheat straw: long-term operation. Bioresour. Technol. 182, 50–57.
Scott, F., Conejeros, R., Aroca, G., 2013. Attainable region analysis for continuous production of second generation bioethanol. Biotechnol. Biofuels 6, 171.
Sumino, H., Takahashi, M., Yamaguchi, T., Abe, K., Araki, N., Yamazaki, S., Shimozaki, S., Nagano, A., Nishio, N., 2007. Feasibility study of a pilot-scale sewage treatment system combining an up-flow anaerobic sludge blanket (UASB) and an aerated fixed bed (AFB) reactor at ambient temperature. Bioresour. Technol. 98, 177–182.
Wang, F., Hidaka, T., Tsuno, H., Tsubota, J., 2012. Co-digestion of polylactide and kitchen garbage in hyperthermophilic and thermophilic continuous anaerobic process. Bioresour. Technol. 112, 67–74.
Wang, L.K., Shammas, N.K., HUNG, Y.-.T., 2007. Biosolids Treatment Processes. Humana Press Inc, New Jersey.
Weiland, P., Rozzi, A., 1991. The start-up, operation and monitoring of high-rate anaerobic treatment systems: discusser's Report. Water Sci. Technol. 24, 257–277.
Zhang, J., Loh, K.-.C., Li, W., Lim, J.W., Dai, Y., Tong, Y.W., 2017. Three-stage anaerobic digester for food waste. Appl. Energy 194, 287–295.